Journal of Magnetism and Magnetic Materials 324 (2012) 3853–3858

Contents lists available at SciVerse ScienceDirect

Journal of Magnetism and Magnetic Materials

journal homepage: www.elsevier.com/locate/jmmm

Investigation on magnetic properties of orientated nanocomposite $Pr_2Fe_{14}B/\alpha$-Fe permanent magnets by micromagnetic finite-element method

Shu-li He [a,b,*], Hong-wei Zhang [b,**], Chuan-bing Rong [b], Juan Chen [a], Ji-rong Sun [b], Bao-gen Shen [b]

[a] Department of Physics, Capital Normal University, Beijing 100037, China
[b] State Key Laboratory of Magnetism, Institute of Physics and Center for Condensed Matter Physics, Chinese Academy of Science, Beijing 100080, China

ARTICLE INFO

Article history:
Received 14 October 2011
Received in revised form
8 June 2012
Available online 3 July 2012

Keywords:
Nanocomposite
Magnetic properties
Micromagnetic finite-element method

ABSTRACT

Demagnetization curves for nanocomposite $Pr_2Fe_{14}B/\alpha$-Fe permanent magnets with different hard grain alignment are calculated by a micromagnetic finite-element method. The results show that both remanence and coercivity increase with improving hard grains alignment. The demagnetization curves show a single-phase demagnetization behavior for the samples with grain size d of 10 nm and two-phase behavior for the samples with d of 20 and 30 nm. H_{ex} (reflecting the magnetic hardening of α-Fe) and H_{irr} (expressing the irreversible reversal of hard phase) are both enhanced with improving the hard grain alignment. The magnetic reversal in orientated nanocomposite permanent magnets is mainly controlled by inhomogeneous pinning of the nucleated type.

1. Introduction

Nanocomposite magnets composed of exchange-coupled hard and soft magnetic phases have attracted much attention due to their high energy products $(BH)_{max}$. Skomski and Coey predicted that the theoretical energy product of $Sm_2Fe_{17}N_3/Fe_{65}Co_{35}$ multilayer might be as high as 120 MG Oe [1]. But up to now, $(BH)_{max}$ of nanocomposite magnets have only achieved about 20 MG Oe [2–4]. There are several difficulties to be overcome: controlling the material structure at the nanoscaled regime, especially to fabricate uniform grain sizes and their soft grain sizes of about 10 nm; aligning the hard magnetic grains sufficiently and ensuring effective exchange coupling between the two phases in all grains through a homogeneous distribution. Nanocomposite magnets prepared by conventional techniques like rapid solidification or mechanical alloying are isotropic and their grain sizes are generally larger than 10 nm. Recently, isotropic nanocomposite FePt/Fe_3Pt with uniform grain sizes of 5 nm was prepared by chemical self-assembly method, which only achieves an energy product of 20.1 MG Oe [5]. Therefore, the crystallite orientation of hard phase is the most important factor to exploit the full magnetic potential of the nanocomposite magnets.

Kato et al. studied the anisotropic nanocomposite magnet in $Nd_2Fe_{14}B/\alpha$-Fe thin film and estimated the intergrain exchange-coupling constant [6]. Many efforts have been made to develop anisotropic nanocomposite magnets in experiment. For the former, fully dense anisotropic nanocomposite R-Fe-B/Fe magnets were prepared by hot pressing and subsequent die upsetting blending of R-rich and R-lean melt-spun ribbons [7,8]. The magnets have layered structure, in which a crystallographic alignment of $R_2Fe_{14}B$ grains is only observed in single-phase layers and exchange-coupled $R_2Fe_{14}B$ and α-Fe grains retain the random crystallographic orientation in two-phase layers. Many studies show that R-rich grain-boundary phase is critical to obtain desired crystallographic texture and therefore $R_2Fe_{14}B$ texture usually appears in R-rich alloys [9,10]. Recently, preferential growth of $R_2Fe_{14}B$ nanocrystals was realized in R-lean alloys by employing a high-pressure technology [11–14]. It should be noted that $R_2Fe_{14}B$ grains were only partially aligned in experimental study. Furthermore, the amount of α-Fe is limited to be lower than 2% vol. because more α-Fe will lead to deterioration of $R_2Fe_{14}B$ crystallographic texture [14]. Control over crystallite orientation of hard phase grains in exchange-coupled magnets is still a challenge to experimentalists.

Numerical methods allow a more detailed understanding of the effect of hard grain alignments, grain size and content of α-Fe on the magnetization reversal process. Micromagnetic finite-element method (FEM) is proved to be effective for the simulation of hysteresis behavior when thermal activation can be ignored [15–18]. In this paper, magnetic properties of the nanocomposite magnets with different easy axes alignment of hard grains are investigated by micromagnetic FEM.

* Corresponding author at: Department of Physics, Capital Normal University, Beijing 100037, China.
** Corresponding author.
E-mail addresses: hsl-phy@163.com, hsl@g203.iphy.ac.cn (S.-l. He), hwzhang@aphy.iphy.ac.cn (H.-w. Zhang).

0304-8853/$ - see front matter Crown Copyright © 2012 Published by Elsevier B.V. All rights reserved.
http://dx.doi.org/10.1016/j.jmmm.2012.06.034

2. Simulation model

There are different numerical schemes in micromagnetism. The static calculation minimizing the energy of the system is widely used to find a magnetization distribution, so it is approved for the simulation of a magnetic hysteresis loop. By means of FEM, the total magnetic Gibbs free energy:

$$G = E_H + E_D + E_k + E_{ex} \tag{1}$$

is minimized with respect to the direction of the spontaneous polarization J_s. Here, E_H is the Zeeman energy in an external field, E_D the dipolar interaction energy, E_k the anisotropy energy and E_{ex} the exchange energy. In numerical calculations, dipolar interaction is taken into consideration by introducing a magnetic vector potential. A more detailed description of the simulation method used has been given in Ref. [19].

Fig. 1 shows the microstructure of two-phase $Pr_2Fe_{14}B/\alpha$-Fe magnet with ideal grain boundary. The sample is composed of 216 irregularly shaped grains with an average diameter from 10 to 30 nm. The 216 grains are in direct contact without any grain boundary phases. The volume fraction of α-Fe varies from 10% to 30%.

For nanocomposite magnets, because magnetocrystalline anisotropy of soft phase is smaller than that of hard phase by a several orders of magnitude, only the crystallographic orientation of hard phase was considered. In the case of uniaxial anisotropy materials, the misalignment of a grain may be described by the angle θ_i between the *c*-axis and the preferred alignment direction $\overline{\theta}$. The degree of orientation is characterized by the standard deviation:

$$\sigma = \frac{1}{N}\sqrt{\sum_{i=1}^{N}(\theta_i - \overline{\theta})^2} \tag{2}$$

Where $\overline{\theta}$denotes the average easy direction of the magnets, θ_i denotes the angle between the local easy axis direction and preferred alignment axis. The external field is applied parallel to the *z*-direction which is identical with the preferred alignment axis, *i.e.* $\overline{\theta} = 0$. In the previous work, influence of grain size on magnetic properties in nanocomposite magnets was studies and Gaussian distribution function was employed to describe grain size distribution [20–22]. It can be used for the reference to employ the Gaussian distribution function to described the distribution of $Pr_2Fe_{14}B$ easy axes in anisotropic magnets:

$$f_{Gauss}(\theta) \sim e^{-\frac{\theta^2}{2\sigma'^2}} \tag{3}$$

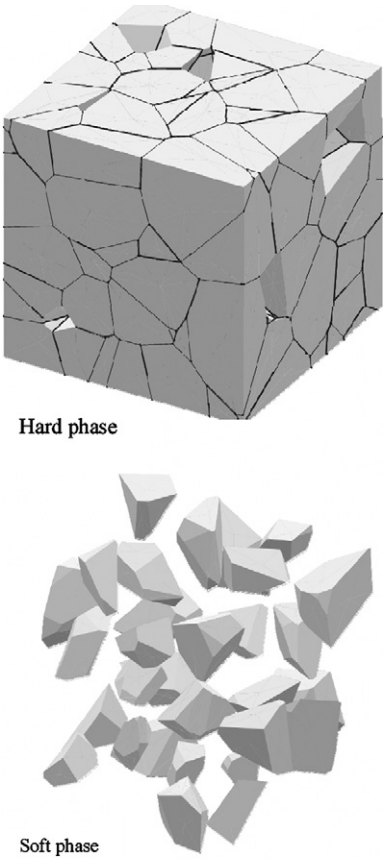

Fig. 1. Microstructure of two-phase $Pr_2Fe_{14}B/\alpha$-Fe magnet consisting of 216 irregular grains with ideal grain boundary, the volume fraction of α-Fe is 20%.

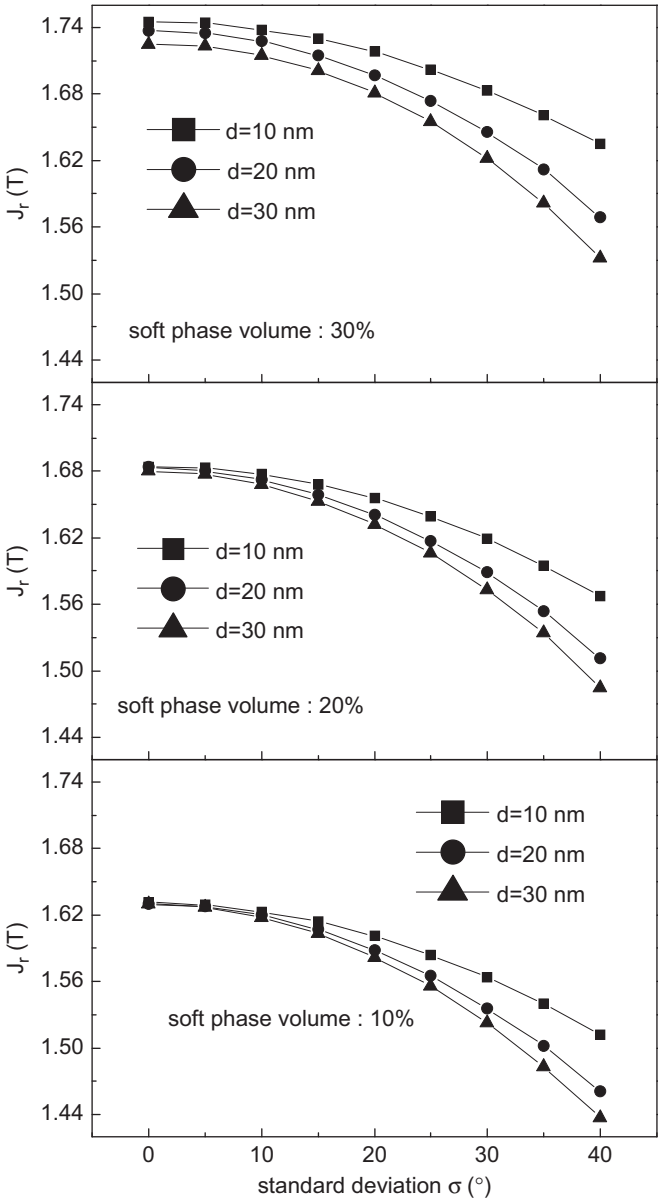

Fig. 2. Dependence of remanence J_r on the standard deviation σ of $f(\theta)$ for $Pr_2Fe_{14}B/\alpha$-Fe nanocomposite magnets.

where σ' is not identical with the standard deviation like usually for Gaussian function because of the cutoff the distribution function for the angles $\theta_i > 90^\circ$.

The magnetic parameters used for the calculation at room temperature are as follow: for α-Fe, $J_s = 2.15$ T, $K_1 = 0.046 \times 10^6$ J/m^3, and $A = 25 \times 10^{-12}$ J/m; for $Pr_2Fe_{14}B$, $J_s = 1.569$ T, $K_1 = 5.567 \times 10^6$ J/m^3, and $A = 7.7 \times 10^{-12}$ J/m. Thus, the Bloch domain wall width of $Pr_2Fe_{14}B$ phase is $\delta_B = 3.7$ nm. In calculations, 75,000–95,000 elements are used.

3. Results and discussion

3.1. A remanence

Fig. 2 shows the dependence of remanence J_r on the standard deviation σ of $f(\theta)$ for nanocomposite magnets with the average grain size d of 10–30 nm and α-Fe content of 10–30 vol% respectively. A continuous decrease of J_r is observed with increasing σ in all the magnets and J_r of magnets with large grains decline more fast than that of the magnets with small grains, which is consistent with the theoretical results for oriented single-phase nanocrystalline permanent magnets [23]. J_r of nanocomposite magnets can be described as $J_r = J_r(h) + J_r(s)$, where $j_r(h)$, results from spontaneous magnetization of hard phase and $J_r(s)$ from that of soft phase. In orientated nanocomposite permanent magnets, remanence enhancement was contributed by both alignment of easy axes in hard grains and intergrain exchange coupling (IGEC) between neighboring hard-hard and hard-soft grains. Improved alignment of easy axes results in increase of magnetization in hard grains paralleling to the external field. In soft magnetic grains with a large spontaneous magnetic polarization, the magnetic moments rotate out of the easy axis more easily than in hard magnetic particles. So, nearly all magnetic moments of the soft magnetic phase align parallel to the average direction of the

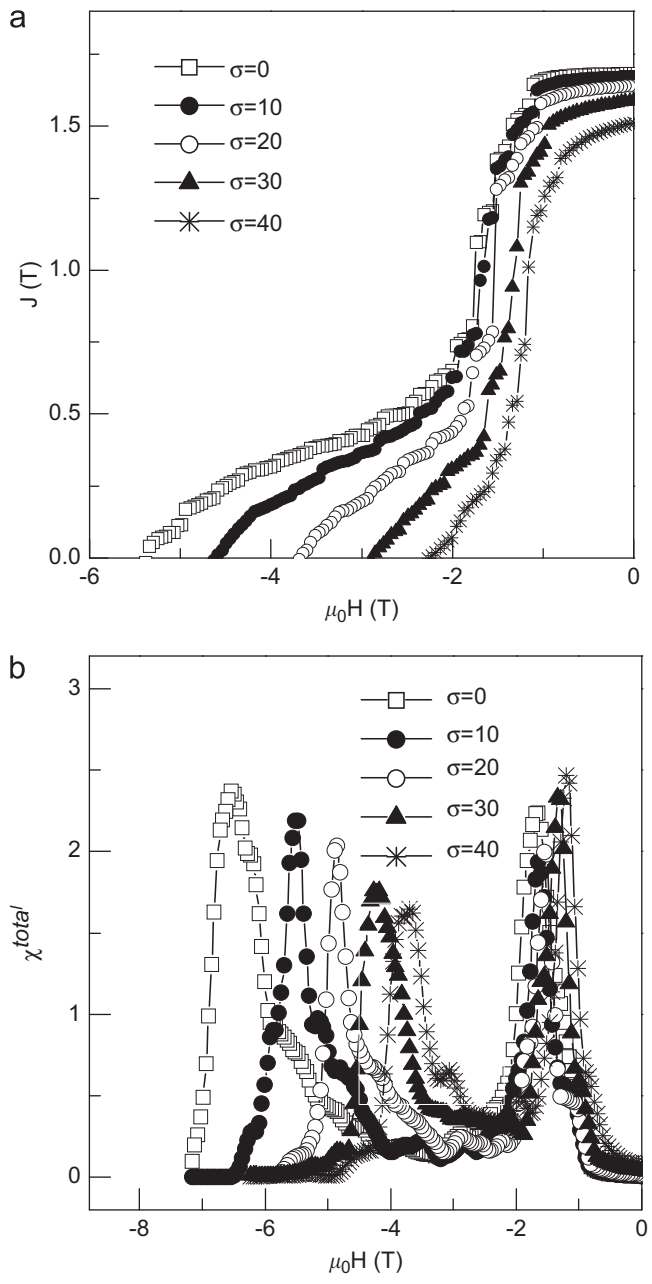

Fig. 3. Demagnetization curves (a) and the corresponding field dependence of total susceptibilities χ^{total} (b) for the magnets containing 20% α-Fe with d of 20 nm.

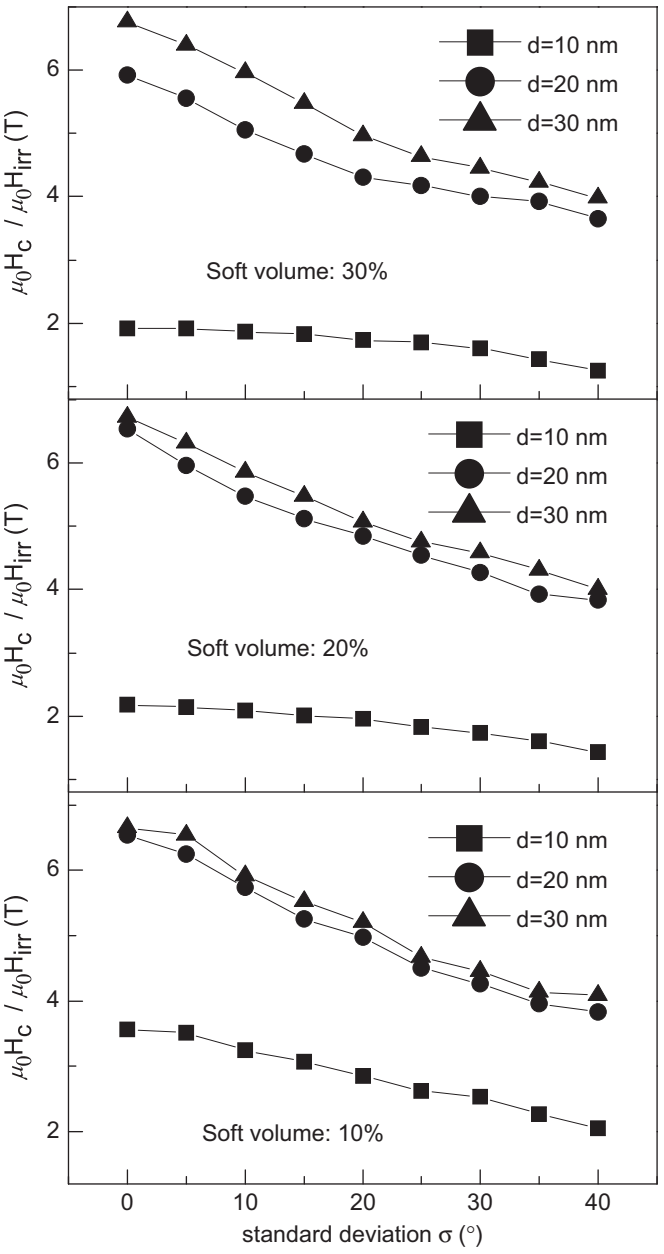

Fig. 4. Dependence of H_c ($d = 10$ nm) and H_{irr} ($d > 10$ nm) on standard deviation σ.

easy axis of the neighboring hard magnetic grains, which causes remanence enhancement. IGEC plays an important role in nanoscaled permanent magnets. IGEC forces magnetization to deviate somewhat from the local easy axis, which causes a smooth transition of magnetization from one easy direction to the other over a width of δ_B and results in remanence enhancement. The smaller the average grain size is, the stronger is IGEC in the magnets. Therefore, it is reasonable that J_r of the nanocomposite increase with decreasing d when σ and α-Fe volume fraction is kept constant, as shown in Fig. 2.

It should be mentioned that, there is little difference among J_r of the magnets with perfectly oriented hard phase containing 10% and 20% α-Fe, whereas an obvious decrease of J_r can be found with increasing grain size in the magnets with perfect crystallographic alignment of hard grains containing 30% α-Fe. Since the magnetization of hard grains is all parallel to the direction of external field, the decline of J_r should be attributed to decreasing magnetization of soft phase. In the case of α-Fe content V_s less than 20%, soft grains are separated from each other by the hard grains in the magnets and no-touching in soft grains is guaranteed [24]. Therefore, soft grains can be exchange coupled completely by hard grains even though d of the magnets is as large as 30 nm. However, it is impossible to guarantee no touched soft grains in our calculation in the case of $V_s \geq 20\%$. The connection of α-Fe grains forms large soft grains. The combined of soft phase grains are too large to be exchange-coupled completely leading to the center of soft grains cannot be exchange coupled. The weaker IGEC, the smaller fraction volume of exchange hardening area in α-Fe is. As a result, it can be easily understood that J_r decreases with increasing d in the nanocomposite magnets containing 30% α-Fe with perfectly oriented hard grains. With α-Fe content increasing from 10% to 30% the remanence of orientated nanocomposite magnets increases monotonically, which is similar to that of isotropic nanocomposite magnets.

3.2. Coercivity

The coercivity field is highly sensitive to microstructural features such as the average grain size, the distribution and volume fraction of the soft magnetic phase, particle shape and the orientation of the easy axis. The calculated results show that the demagnetization curves show a single-phase behavior for $d=10$ nm and a two-phase behavior for $d>10$ nm, which is coincide with the experimental results [25,26]. It is suggested that more information on magnetization reverse can be obtained from the plot of χ^{total} *versus* H for two-phase behavior magnets [27]. Fig. 3 shows demagnetization curves and the corresponding field dependence of total susceptibilities χ^{total} for the magnets containing 20% α-Fe with d of 20 nm. For convenience, we defined the exchange bias field H_{ex} as the field in which the first maximum χ^{total} is obtained and the irreversible reverse field H_{irr} as the field in which the last maximum χ^{total} reached. Both are different from coercivity H_c where magnetization is zero. Thus, for single-phase behavior magnets, $H_{\rm irr}=H_{\rm ex}=H_{\rm c}$, and for two-phase behavior magnets, the demagnetization behavior is not well characterized by H_c but by H_{ex} and H_{irr}. The value of H_{ex} depends on soft-hard IGEC, and is equal to the magnetocrystalline anisotropy field of hard phase as the soft layer width is less than $2\delta_B$ in multilayer thin film [1,28,29]. The first maximum χ^{total} shown in Fig. 3 is attributed to the spring like reversal of α-Fe phase. Fig. 3

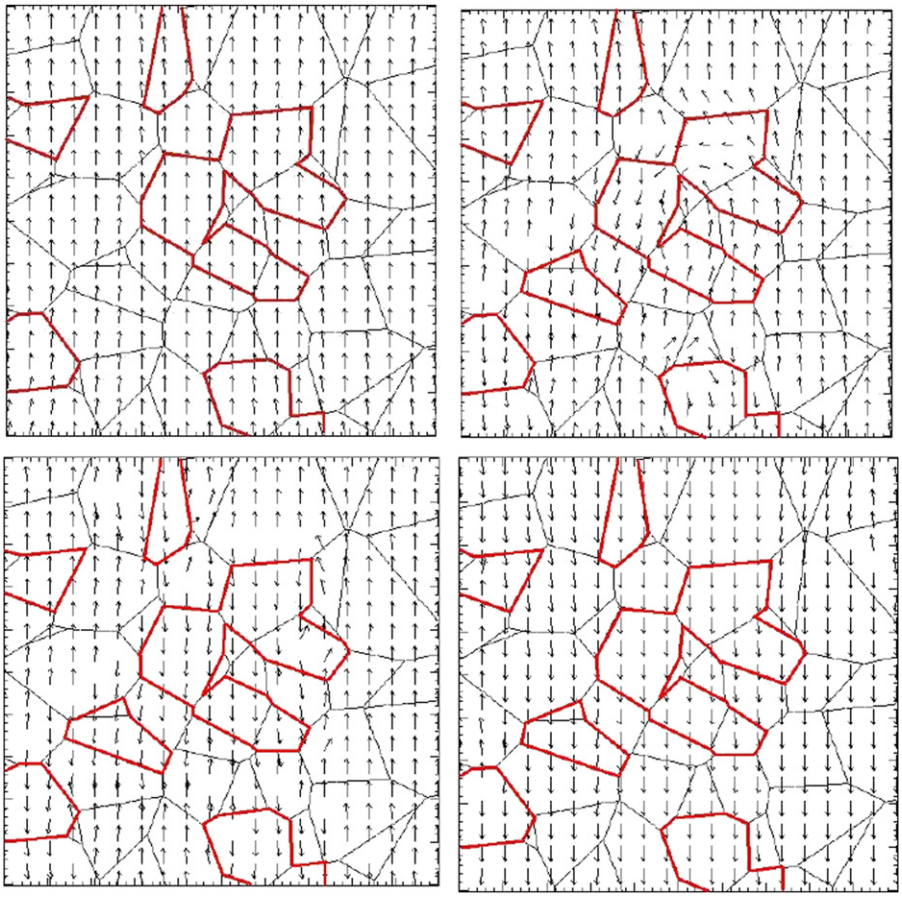

Fig. 5. Magnetization vector in demagnetization process of perfectly oriented nanocomposites with 20% soft phase. The area enclosed by red line represents soft grains.

shows that H_{ex} is slightly enhanced with improved hard grains alignment, whereas an H_{irr} significantly moves towards high field with decreasing σ. In nanocomposites, the magnetic moments rotated out of the easy axis more easily than in hard magnetic particles and parallel to the average direction of the easy axis of the neighboring hard magnetic grains. Therefore, improvement of hard grains alignment leads to an increase of magnetic moment in soft grains which parallel to z-axis.

Fig. 4 shows the dependence of $H_c(d=10\ \text{nm})$ and $H_{irr}(d>10\ \text{nm})$ on σ. H_c or H_{irr} increases monotonically with improved hard grains alignment, which is similar to that of non-interaction system. Fig. 5 describes the magnetization vector in demagnetization process of perfectly oriented nanocomposites with 20% soft phase. Here, we would like to use one-dimension model proposed by Keneller and Hawig [28] to interpret the demagnetization process of nanocomposite magnets. Starting from the saturation remanence along easy axis direction, magnetization changes reversibly in the soft phase with increasing reverse field and two equilibrium 180° walls form. These wall are reversibly compressed towards the hard phase with increasing reverse field. The nucleated domains are pinned at the neighboring hard phase grain boundary in the case of applied field $H \cdot H_{irr} > H > H_{ex}$. The energy density in these walls $E_{\gamma m}$ increases above its equilibrium value $E_{\gamma 0m}$ continuously with increasing H. When H further increases up to H_{irr}, approaches to the equilibrium energy density of a wall in hard phase $E_{\gamma 0s}$, the first reversed domain walls invade into hard phase and irreversible reversion takes place. Therefore, the mechanism of magnetic reversal is dominantly determined by the inhomogeneous pinning of nucleated type.

4. Maximum energy product

Fig. 6 demonstrates maximum energy product $(BH)_{max}$ as a function of σ with $d=10$–30 nm, $V_s=10$–30%. $(BH)_{max}$ increase monotonically with improved hard grain alignment. Because of low α-Fe concentration and aligned hard grains in the calculated magnets, H_c is much higher than one half of the remanence, $(BH)_{max}$ sensitively depends on the remanence. For perfectly orientated magnets with 10% α-Fe, $(BH)_{max}$ is not sensitive to d, which is in a good agreement with the results of Fig. 2. As V_s is constant, the magnets with small d exhibit high remanence, which leads to high $(BH)_{max}$. Therefore, in this paper, perfectly orientated magnets containing 30% α-Fe with d of 10 nm exhibits the highest $(BH)_{max}$ of about 600 KJ/m^3.

It is noticeable that the effect of α-Fe content on $(BH)_{max}$ sensitively depends on d of the magnets. For $d=10$ nm, the magnets with 30% α-Fe show highest $(BH)_{max}$ and that containing 10% α-Fe lowest $(BH)_{max}$. With d increasing to 30 nm, the magnets with 10% α-Fe exhibit highest $(BH)_{max}$ and that with 30% α-Fe lowest $(BH)_{max}$. Fig. 6 suggestes that, small grain size and relatively high soft phase content are of benefit to high $(BH)_{max}$ for ideally orientated nanocomposite magnets. However, as Vs is too large, the soft grains connected to each other forming big soft grains, the stray field plays a dominant role and forces the magnetization of soft grain to form vortex flow, which leads to a drastic decrease of J_r and $(BH)_{max}$.

5. Conclusion

The influence of crystallographic orientation of hard phase on magnetic properties of nanocomposites were investigated systematically. The remanence of nanocomposites increases with improving hard grains alignment. The demagnetization behavior of nanocomposites possessing a two-step demagnetization behavior should be characterized by H_{ex} which reflects the magnetic hardening of α-Fe and H_{irr} which expresses the irreversible reversal of hard phase instead of H_c. With improved hard grains alignment, H_{ex} and H_{irr} both increase monotonically. An ordered crystallographic orientation of hard grains can lead to a significant increase of $(BH)_{max}$. Our results of magnetization vector in demagnetization process give a direct evidence that the magnetic reversal in the nanocomposites magnets is mainly controlled by in homogeneous pinning of nucleated type, which was proposed by us before. A maximum energy product as high as about 75 MGOe is predicted in this paper, which is much higher than the experimental data up to now. Highly ordered orientation of hard phase is the critical factor to improve the properties of nanocomposites. It is still challenging for experimentalists to obtain strong texture of hard grains in the nanocomposites in which the amount of α-Fe keeps a relatively high level.

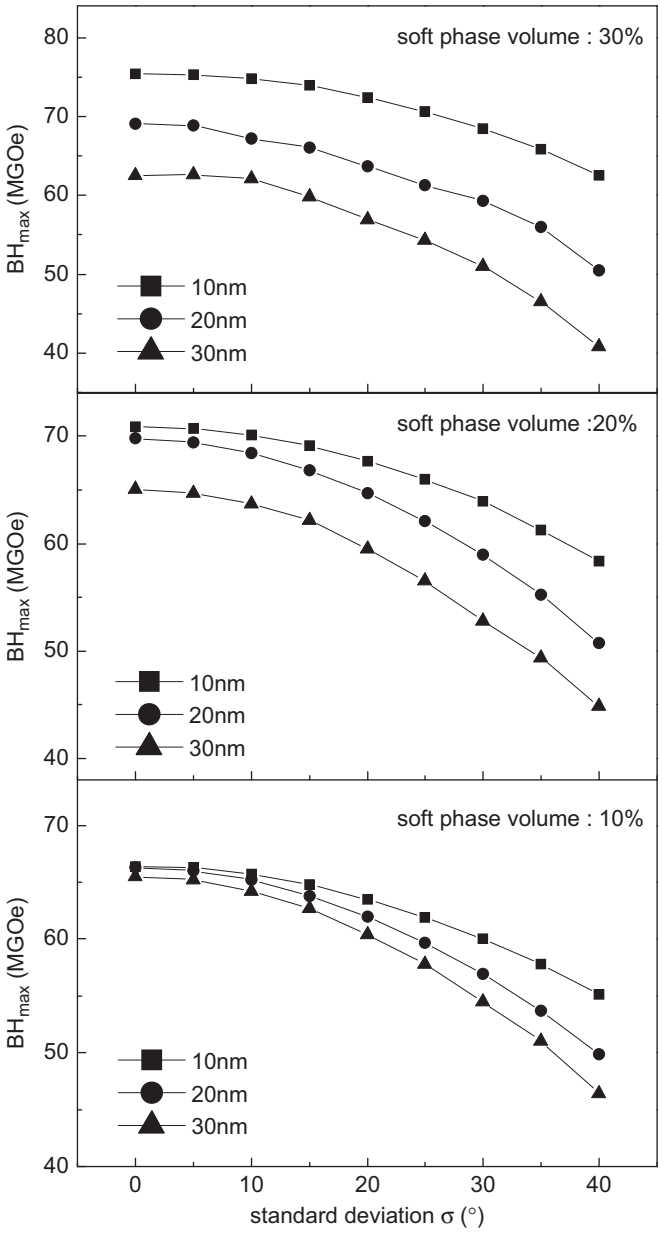

Fig. 6. Maximum energy product $(BH)_{max}$ as a function of standard deviation σ.

Acknowledgments

This work is supported by the National Natural Science Foundation of China(Grant no. 51171121).

References

[1] R. Skomski, J.M.D. Coey, Physical Review B 48 (1993) 15812.
[2] A. Manaf, R.A. Buckley, H.A. Davies, Journal of Magnetism and Magnetic Materials 128 (1993) 302.
[3] D. Goll, M. Seeger, H. Kronmuller, Journal of Magnetism and Magnetic Materials 185 (1998) 49.
[4] X.B. Du, H.W. Zhang, C.B. Rong, J. Zhang, S.Y. Zhang, B.G. Shen, Y. Yu, H.M. Jin, Journal of Magnetism and Magnetic Materials 271 (2004) 396.
[5] H. Zeng, J. Li, J.P. Liu, Z.L. Wang, S.H. Sun, Nature 420 (2002) 395.
[6] H. Kato, M. Ishizone, K. Koyama, T. Miyazaki, Journal of Magnetism and Magnetic Materials 290-291 (2005) 1221.
[7] D. Lee, J.S. Hilton, S. Liu, Y. Zhang, G.C. Hadjipanayis, C.H. Chen, IEEE Transactions on Magnetics 39 (2003) 2947.
[8] A.M. Gabay, Y. Zhang, G.C. Hadjipanayis, Applied Physics Letters 85 (2004) 446.
[9] D. Lee, S. Bauser, A. Higgins, C. Chen, S. Liu, M.Q. Huang, Y.G. Peng, D.E. Laughlin, Journal of Applied Physics 99 (2006) 08B516.
[10] A.M. Gabay, M. Marinescu, G.C. Hadjipanayis, Journal of Applied Physics 99 (2006) 08B506.
[11] W. Wu, W. Li, H.Y. Sun, H. Li, X.H. Li, B.T. Liu, X.Y. Zhang, Nanotechnology 19 (2008) 195010.
[12] B.Y. Liang, Y.W. Xie, W. Li, W. Wu, X.Y. Zhang, Journal of Physics D: Applied Physics 41 (2008) 195010.
[13] Y.G. Liu, L. Xu, Q.F. Wang, W. Li, X.Y. Zhang, Applied Physics Letters 94 (2009) 172502.
[14] M. Yue, P.L. Niu, Y.L. Li, D.T. Zhang, W.Q. Liu, J.X. Zhang, C.H. Chen, S. Liu, D. Lee, A. Higgins., Journal of Applied Physics 103 (2008) 07E101.
[15] R. Fischer, T. Leineweber, H. Kronmuller, Physical Review B57 (1998) 10723.
[16] H. Kronmuller, R. Fischer, M. Bachmann, T. Leineweber, Journal of Magnetism and Magnetic Materials 203 (1999) 12.
[17] R. Fischer, H. Kronmuller, Journal of Applied Physics 83 (1998) 3271.
[18] H.W. Zhang, C.B. Rong, X.B. Du, S.Y. Zhang, B.G. Shen, Journal of Magnetism and Magnetic Materials 278 (2004) 127.
[19] R. Fischer, H. Kronmuller, Physical Review B54 (1996) 7284.
[20] H. Kronmüller, K.-D. Durst, G. Martinek, Journal of Magnetism and Magnetic Materials 69 (1987) 149–157.
[21] G. Rieger, M. Seeger, H. Kronmüller, Physica Status Solidi (a) 583 (1999) 171.
[22] J. Bauer, M. Seeger, A. Zern, H. Kronmüller, Journal of Applied Physics 80 (3) (1996) 1667.
[23] S.L. He, H.W. Zhang, C.B. Rong, R.J. Chen, J.R. Sun, B.G. Shen, Acta Physica Sina 54 (2005) 3408.
[24] C.B. Rong, H.W. Zhang, X.B. Du, J. Zhang, S.Y. Zhang, B.G. Shen, Journal of Applied Physics 96 (2004) 7.
[25] W.Y. Zhang, C.B. Rong, J. Zhang, B.G. Shen, H.L. Du, J.S. Jiang, Y.C. Yang, Journal of Applied Physics 92 (2002) 7647.
[26] H. Chiriac, M. Marinescu, K.H.J. Buschow, F.R. de Boer, E. Bruck, Journal of Magnetism and Magnetic Materials 202 (1999) 22.
[27] H.W. Zhang, T.Y. Zhao, C.B. Rong, S.Y. Zhang, B.S. Han, B.G. Shen, Journal of Magnetism and Magnetic Materials 267 (2003) 224.
[28] E.F. Kneller, R. Hawig, IEEE Transactions on Magnetics 27 (1991) 3588.
[29] M. Amato, A. Rettori, M.G. Pini, Physica B 275 (2000) 120.